Journal of Applied Polymer Science

Synthesis, Helical Conformation, and Infrared Emissivity Property Study of Optically Active Substituted Polyacetylenes Derived from Serine

Xiaohai Bu, Yuming Zhou, Tao Zhang, Man He, Yongjuan Wang
School of Chemistry and Chemical Engineering, Southeast University, Jiangsu Optoelectronic Functional Materials and Engineering Laboratory, Nanjing 211189, People's Republic of China
Correspondence to: Y. Zhou (E-mail: ymzhou@seu.edu.cn)

ABSTRACT: Serine-based monosubstituted acetylene monomers were synthesized and polymerized with rhodium zwitterion catalyst in THF to afford optically active polyacetylene derivatives (LPA and DPA) and corresponding racemic polyacetylenes (RPA) with moderate molecular weights in good yields. All of the substituted polyacetylenes (SPA) were characterized by FT-IR, NMR, GPC, UV-Vis spectroscopy, circular dichroism (CD) spectroscopy, and TGA. LPA and DPA were soluble in common organic solvents and possessed single-handed helical conformation according to their intense Cotton effect and large specific rotations, while RPA presented random coiled polymer chain. The characterization results showed that helical structure of these SPAs was stabilized by intra- and intermolecular hydrogen bonding between the substituents which played a significant role in creating and maintaining the helix. Further, the infrared emissivity properties of them at wavelength of 8 to 14 μm were investigated at room temperature. Consequently, the LPA and DPA exhibited lower infrared emissivity values than RPA, which came down to 0.632 and 0.616. © 2014 Wiley Periodicals, Inc. J. Appl. Polym. Sci. **2015**, *132*, 41210.

KEYWORDS: applications; optical properties; properties and characterization; stimuli-sensitive polymers

Received 10 May 2014; accepted 24 June 2014
DOI: 10.1002/app.41210

INTRODUCTION

In recent years, materials with low infrared emissivity have attracted great attention due to their potential applications in thermal insulation and military stealthy.[1,2] Semiconductor and metallic materials have been widely exploited to achieve low emissivity owing to the high reflectance of them in infrared waveband.[3–5] Many organic polymers possess relatively high emissivity (commonly larger than 0.90) because of the presence of highly absorptive bonds such as amide, amino and hydroxyl groups. However, these polymers possess unique properties including low density, tractability, anti-corrosion and the most value, their adjustable composition and structure, which provide intriguing possibility of adjusting their performance efficaciously according to practical applications. Therefore, developing novel polymers with low infrared emissivity has remained a meaningful research objective.

Helix is one of the most common structures in naturally occurring biomacromolecules such as polypeptide, DNA, and proteins, which predominantly prefers single-handed screw sense. Helical structures are primarily constructed through intra- and/or intermolecular associations by noncovalent forces, such as hydrogen bonding, hydrophobic-stacking, and electrostatic interactions. To date, considerable effort is devoted to the syntheses and conformation studies of synthetic polymers with helical conformations, including polyacetylenes, poly(alkylmethacrylates), polychloral, polyisocyanates, polyisocyanides, polysilanes, and so forth.[6–9] Some of them are proved to be capable of undergoing conformational transitions by external stimuli which endow the macromolecule with a two-state "on-off" function, thus making them useful in fabricating molecular switches, data storage devices and smart polymeric materials. Especially, synthesis of amino acid and peptide-containing polymers is a topic of much interest because of their potential properties such as biocompatibility, biodegradability, and unique optical properties based on their higher order secondary structures. In the case of organic infrared low-emissive polymers, considerable effort has been devoted to applying helical polymers in this field owing to their adjustable secondary structure. For example, Wang et al.[10] firstly reported that optically active polyurethane-urea had a lower infrared emissivity value compared with racemic polymers because of its ordered

Additional Supporting Information may be found in the online version of this article.

single-handed conformation. Yang et al.[11,12] synthesized optically active polyurethanes with lower emissivity values and studied the correlation between the helical structure and infrared emission. According to their work, well-ordered structure seems to be efficient in decreasing the infrared emissivity, despite the presence of some unfavorable absorptive groups in synthetic polymers. The vibration of unsaturated functional groups mainly brings about the high infrared radiation. In principle, compact accumulation of fragments and orderly molecular interactions will accelerate the change of vibrational state of unsaturated bonds to influence the thermal restraining in backbones. Namely, a high-ordered helical structure, to some extent, can change the vibration mode of the whole macromolecular to reduce the index of hydrogen deficiency and the unsaturated degree, thus eventually facilitating the decrease in infrared emissivity values.

Polyacetylene is the simplest linear conjugated macromolecule and is a typical conductive polymer. Due to its rigidly π-stacked main chain, it is infusible and insoluble in any kind of solvent. However, substituted polyacetylene (SPA) not only possesses the properties of common polymers, but also shows great potential in optoelectronics, catalyst, stimuli-responsive materials, gas separation, etc.[13–16] Previous researches have been conducted on the synthesis of SPAs carrying functional substitutes using metal carbene and metal halide catalysts. Especially, many studies have focused on SPAs derived from chiral amino acids as candidates because they exhibit biocompatibility, biodegradability, optical activity, and diverse active functional groups.[17–20] The amino acid-based moieties at the pedants compete with each other and their chiral information is transmitted to the polymer backbone, leading to dynamic helical secondary structures of SPA chains. A wide variety of helical SPAs derived from chiral amino acid have been designed and synthesized. Zhao et al.[21] synthesized SPA derived from various amino acids and studied their conformational transition by changing temperature and solvent. Li et al. also synthesized helical poly(phenylacetylenes) carrying amino acid moieties, some of which exhibit interesting molecular properties.[22,23] It is important to point out that the sense, tightness, and stability of their helical structures depend on the functional groups in the pendants such as amide, hydroxyl, and aromatic groups. Especially, hydroxyl group forms hydrogen bonding in a different way which can not only assist to form hydrogen bonds but also have great effect in stabilizing the helix.[24,25] Participation of hydroxyl group in intramolecular hydrogen bonding changes the torsional angles in the main chain. This finding is significant for further fabrication of hydroxyl group-containing helical SPAs for special applications, for instance, SPAs for tunable infrared emissivity application.

To our knowledge, there are also few reports concerning the application of helical polymers to achieve tunable infrared emissivity, let alone helical SPAs. Herein, SPAs derived from chiral and racemic serine was designed and synthesized. Hydroxyl groups in serine are incorporated for the formation of hydrogen bonds and stabilization of helix. As structurally composition of the polymer varies, the change of hydrogen bonding and chain helicity can afford the SPAs with different performance in controlling infrared emission. The testing results demonstrate that optically active SPAs (LPA and DPA) possess lower infrared emissivity values than the racemic one, which may be attributed to the incorporation of the chirality in the resulting SPA chains.

EXPERIMENTAL

Materials

Propargylamine, *N-tert*-butoxycarbonyl-L-serine and *N-tert*-butoxycarbonyl-D-serine were supplied by Aladdin. $[(nbd)RhCl]_2$ (nbd = 2,5-norbornadiene) was purchased from Acros Organics. Isobutyl chloroformate and 4-methymorpholine were purchased from Sinopharm Chemical Reagent Co., Ltd. $(nbd)Rh^+[\eta^6\text{-}C_6H_5B^-(C_6H_5)_3]$ was prepared by the reaction of $[(nbd)RhCl]_2$ with $NaB(C_6H_5)_4$ as described in the literature.[26] THF used for polymerization was distilled over CaH_2 prior to use. All other regents were used as received without further purification.

Measurements

Melting point (mp) was measured by an X-4 micro-melting point apparatus. FT-IR spectra were carried out on a Bruker Tensor 27 FT-IR spectrometer at room temperature. Solution FT-IR spectra were obtained by using chloroform as solvent in a KBr liquid cell. The spectra were obtained at a 4 cm^{-1} resolution and recorded in the region of 4000-400 cm^{-1}. ^1H and ^{13}C NMR spectra measurements were recorded on a Bruker AVANCE 300 NMR spectrometer. Chemical shifts were reported in ppm. The molecular weights and molecular weight polydispersities were estimated by gel permeation chromatography (Shodex KF-850 column, THF as the eluent, polystyrene calibration). UV-Vis spectra were measured on a Shimadzu UV-3600 spectrometer. CD spectra were determined with a Jasco J-810 spectropolarimeter using a 10 mm quartz cell at room temperature. Specific rotations ($[\alpha]_D$) were measured in a WZZ-2S (2SS) digital automatic polarimeter at room temperature. Thermal analysis experiments were performed using a TGA apparatus operated in the conventional TGA mode (TA Q-600, TA Instruments) at the heating rate of 10 K min^{-1} in a nitrogen atmosphere, and the sample size was about 5 mg. The infrared emissivity values (ε) of polymers at wavelength of 8 to 14 μm were investigated on the IRE-2 Infrared Emissometer of Shanghai Institute of Technology and Physics, China. Infrared emissivity values of the samples at 20 to 160°C were recorded with a temperature control instrument at a heating rate of 5 K min^{-1}.

Monomer Synthesis

N-tert-butoxycarbonyl-L-serine (1.125 g, 5.5 mmol), isobutyl chloroformate (0.72 mL, 5.5 mmol), and 4-methymorpholine (0.6 mL, 5.5 mmol) were sequentially added into THF (35 mL) and stirred at room temperature for about 15 min. Then, propargylamine (0.303 g, 5.5 mmol) was added into the mixture and stirred at 25°C for 24 h. The white precipitate was filtered off, and the filtrate was collected, to which AcOEt (200 mL) was added to extract the desired product. The combined solution was subsequently washed with 1*M* HCl, saturated $NaHCO_3$ (aq.), and saturated NaCl (aq.) three times. The organic layer was dried over anhydrous $MgSO_4$ and concentrated by rotary evaporation. The residue was purified by recrystallization from *n*-hexane and AcOEt to obtain *N-tert*-butoxycarbonyl-L-serine-*N*'-propargylamide (LS) solid product. In a similar way, *N-tert*-butoxycarbonyl-D-serine-*N*'-propargylamide (DS) and

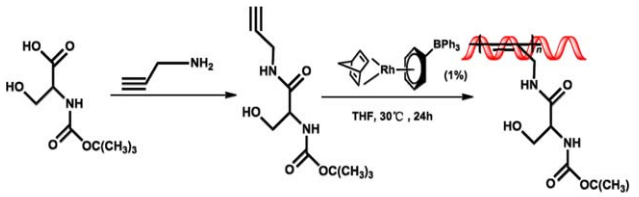

Scheme 1. Synthesis of the SPAs. [Color figure can be viewed in the online issue, which is available at wileyonlinelibrary.com.]

their racemic monomer (RS) were synthesized using *N-tert*-butoxycarbonyl-D-serine and *N-tert*-butoxycarbonyl-D,L-serine instead of *N-tert*-butoxycarbonyl-L-serine.

LS: Yield = 62%, mp: 156–158°C. $[\alpha]_D = 5.9°$ ($c = 0.1$ g/dL, THF, rt). FT-IR (cm^{-1}, KBr): 3455, 3330, 3303, 3096, 1710, 1662, 1570, 1536, 1410, 1365, 1283, 1249, 1174, 1058, 1046, 930, 863, 785, 659, 526. ^{1}H NMR (300 MHz, $CDCl_3$): δ 1.49 [s, 9H, $(CH_3)_3$], 2.25 (s, 1H, C≡C**H**), 2.92 (s, 1H, CH_2OH), 3.68 (s, 1H, CH_2CHNH), 4.09 (s, 2H, $CHCH_2OH$), 4.17 (m, 2H, CH_2NH), 5.58 (s, 1H, CHN**H**CO), 7.00 (s, CH_2NHCO). ^{13}C NMR (75 MHz, $CDCl_3$): δ 28.30, 29.35, 56.50, 62.89, 71.74, 79.03, 80.99, 157.82, 171.28.

DS: Yield = 51%, mp: 156–159°C. $[\alpha]_D = -6.0°$ ($c = 0.1$ g/dL, THF, rt). Its ^{1}H NMR, ^{13}C NMR and FT-IR data are similar to LS and thus omitted.

RS: Yield = 67%, mp: 168–171°C. $[\alpha]_D = 0°$ ($c = 0.1$ g/dL, THF, rt). Its ^{1}H NMR, ^{13}C NMR and FT-IR data are similar to LS and thus omitted.

Polymerization of Substituted Polyacetylenes

Polymerizations were carried out in a Y-type glass tube equipped with a three-way stopcock under nitrogen. Monomers and $(nbd)Rh^+[\eta^6\text{-}C_6H_5B^-(C_6H_5)_3]$ ([initial monomer] = 0.5*M*, [Rh catalyst] = 0.005*M*) were respectively dissolved in THF under N_2 atmosphere. The monomer and catalyst were then mixed and stirred at 30°C for 24 h. After polymerization, the resultant solution was added dropwise into a large amount of *n*-hexane/AcOEt (10/1, v/v) to precipitate the formed polymers. The precipitate was collected by filtration and dried under reduced pressure to obtain the SPA products. SPA polymerized from LS, DS and RS were recorded as LPA, DPA and RPA, respectively.

The spectroscopic data of the as-prepared SPA product is given as follows (take LPA for example). FT-IR (cm^{-1}, KBr): 3600–3200, 3006, 2980, 2930, 2884, 1698, 1658, 1523, 1459, 1399, 1367, 1256, 1169, 1065, 918, 858, 782, 591; ^{1}H NMR (300 MHz, $CDCl_3$): δ 1.45 [br, 9H, $(CH_3)_3$], 3.13 (br, 1H, CH_2OH), 3.1–5.0 (m, 5H, CH_2CHNH, $CHCH_2OH$, CH_2NH), 6.19 (br, 2H, CHN**H**CO, C=C**H**), 7.95 (br, 1H, CH_2NHCO). The ^{1}H NMR and FT-IR data of RPA and DPA are similar to LPA and thus omitted.

RESULTS AND DISCUSSION

Synthesis of Monomers and Polymers

The synthetic route for the *N*-propargylamide monomers used in the polymerization is illustrated in Scheme 1. They were prepared by the reaction of corresponding BOC-protected serine with propargylamine using isobutyl chloroformate and 4-methymorpholine as a condensing agent. The crude products were obtained quantitatively in every case and then were purified by recrystallization in hexane/AcOEt (1/3, v/v). The structures of them were confirmed by NMR and FT-IR spectroscopies and shown in Figure 1 and Supporting Information Figure S1.

Scheme 1 and Table I summarize the conditions and results of the polymerization of DS, LS and RS catalyzed by an Rh catalyst in distilled THF at 30°C for 24 h. The monomers satisfactorily underwent homopolymerization and quantitatively transformed into the corresponding homopolymers with moderate molecular

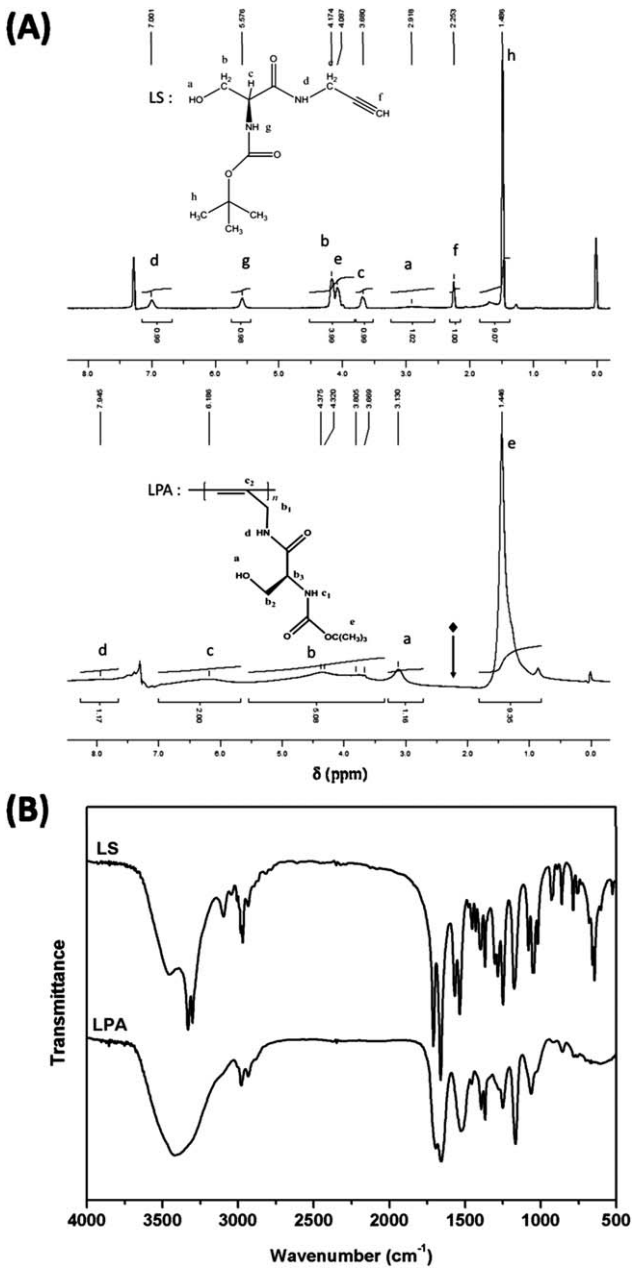

Figure 1. (A) ^{1}H NMR and (B) FT-IR spectra of LS and LPA.

Table I. Polymerization of Serine-Derived SPAs[a]

Polymer	Yield[b] (%)	M_n[c]	M_w/M_n	$[\alpha]_D$[d](°)		
				$CHCl_3$	THF	MeOH
LPA	92	10,100	2.0	−152	−269	−456
DPA	90	10,700	2.2	+165	+275	+488
RPA	95	9900	2.5	0	0	0

[a] Conditions: catalyst (nbd)$Rh^+[\eta^6$-$C_6H_5B^-(C_6H_5)_3]$, [monomer]/[catalyst] = 100, at 30°C for 24 h under nitrogen.
[b] Insoluble part in *n*-hexane/AcOEt (10/1, v/v).
[c] Determined by GPC eluted with THF based on polystyrene standards.
[d] Measured in $CHCl_3$, THF, and MeOH by polarimetry at room temperature, c = 0.05 g dL^{-1}.

Table II. Solubility of Serine-Derived SPAs[a]

Solvent	LPA	DPA	RPA
MeOH	++	++	++
$CHCl_3$	++	++	+
AcOEt	+	+	+
THF	++	++	++
DMF	++	++	++
DMSO	++	++	++
Acetone	+	+	+
n-Hexene	−	−	−
Water	−	−	−

[a] The solubility was measured at a concentration of 10 wt % SPA solid content.
++: diffluent; the solid polymer was quickly dissolved in the solvent to afford a homogenous solution without heating or stirring. +: soluble; the solid polymer was completely dissolved in the solvent to afford a clean solution with stirring. −: insoluble; the solid polymer did not dissolve in the solvent even with heating.

weights (M_n = 9900–10,700). The solubility of serine-derived SPA was tested in various organic solvents, and the results were listed in Table II. The polymers were soluble in common organic solvents including MeOH, $CHCl_3$, AcOEt, THF, DMF, DMSO, and acetone, but were insoluble in *n*-hexane and water.

The composition and structure of corresponding SPAs were examined by FT-IR and ^{1}H NMR spectroscopies, as shown in Figure 1 and Supporting Information Figure S2. As can be seen, for the obtained SPAs, the disappearance of the chemical shift assigned to the acetylene proton at ~2.25 ppm in the spectra of the SPA indicated that the serine-derived monomers had been consumed by the polymerization reaction. Meanwhile, the peaks corresponding to the resonances of the protons of the polyene backbone were hardly recognized for the broad proton signals around 4 to 6 ppm. Since Rh zwitterion complex commonly gives SPA with high stereoregularity (cis), we assume that the steric structures of the present polymers are also this case.[27]

Hydrogen Bonding Analysis

Hydrogen bonds are an essential and fundamental interaction to form and maintain the secondary helical structure for amino acid-based SPAs, especially for SPA containing hydroxyl group. Participation in hydrogen bonding decreases the frequency of free N-H and C=O vibrations but increases the intensities, making the absorption features useful in analyzing hydrogen bonds. The solution state FT-IR spectra of the monomer and as-prepared polymer samples in $CHCl_3$ are examined to determine the existence of hydrogen bonding in the SPAs and shown in Figure 2. As can be seen, for LS, the absorption peaks at 3433 and 3310 cm^{-1} assigned to the free N-H and hydrogen bonded N-H groups can be observed, at, while two broad absorption peaks centered at 1701 and 1668 cm^{-1} are corresponded to the amide C=O and carbamate C=O groups. In Figure 2(A), the bands of free N-H groups for SPAs decreases and the peak intensities corresponded to hydrogen bonded N-H undergo remarkable increase, indicating that a large number of the free N-H groups have converted to be hydrogen bonded. Compared with optically active LPA and DPA, the absorption band of the hydrogen bonded N-H peak in RPA is much weaker. This phenomenon shows that the amounts of free and hydrogen bonded N-H groups in optically active and racemic SPAs are different. This probably originates from the slightly different degrees of hydrogen bonding in these chiral and achiral polymers. In Figure 2(B), the bands of amide C=O and carbamate C=O groups undergoes blue-shift to about 1693 and 1653 cm^{-1}, respectively. From the obvious frequency decease of

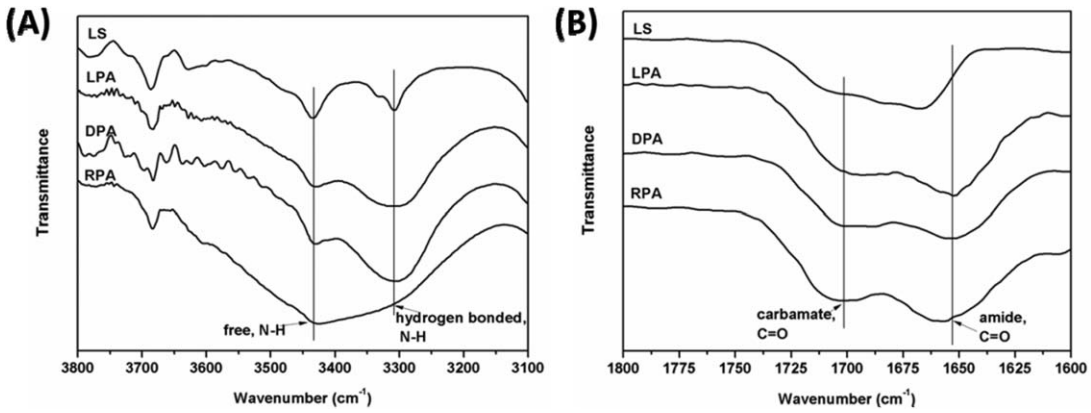

Figure 2. Solution FT-IR spectra of LS, LPA, DPA, and RPA in $CHCl_3$ (A) at 3800 to 3100 cm^{-1} and (B) at 1800 to 1600 cm^{-1}. The concentration of each tested sample is about 0.5 m*M*.

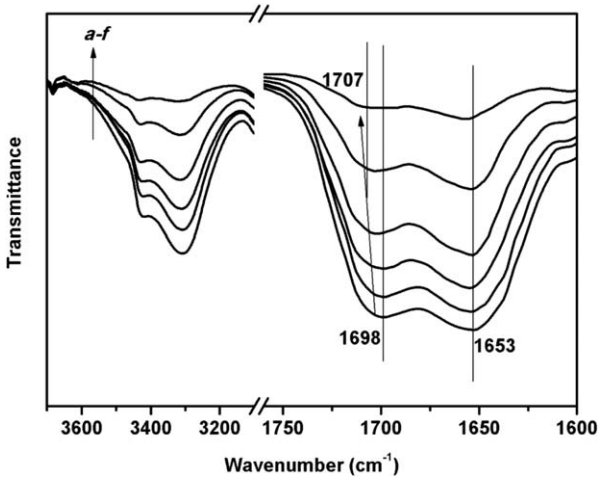

Figure 3. Solution FT-IR spectra of LPA in $CHCl_3$ at the concentrations of (A) 1 m*M*, (B) 0.75 m*M*, (C) 0.5 m*M*, (D) 0.25 m*M*, (E) 0.1 m*M*, and (F) 0.05 m*M*.

the both carbonyl groups, it can be concluded amide and carbamate groups are participated in the formation of inter- and/or intramolecular hydrogen bonds in these SPAs. This is also in good agreement with the N-H absorption features at high frequency band.

To further demonstrate the actual kind of formed hydrogen bonds, the solution FT-IR spectra of LPA at different concentrations are also conducted in $CHCl_3$ as an example. As can be seen in Figure 3, with the decrease of the concentrations from 1 to 0.05 m*M*, the intensities of the band assigned to hydrogen bonded N-H groups decreased together with the increase of free N-H groups, indicating the disappearance of intermolecular hydrogen bonding. For carbonyl groups, the absorption bands of them also became narrower. An obvious red-shift from 1698 to 1705 cm^{-1} of the band corresponding to carbamate C=O groups was observed upon the decreasing concentration, while no obvious frequency change occurred at the band of amide C=O. Therefore, it can be inferred that most of carbamate groups are probably participated in the formation of intermolecular hydrogen bonds, while the inner amide groups prefer to form intramolecular hydrogen bonds in the SPA chains. Moreover, even at such low concentrations, still high degree of intramolecular hydrogen bonding constructed by amide C=O groups existed, also demonstrating the role of amide groups in formation of intramolecular hydrogen bonds. Summarizing the observations in the FT-IR spectra, it is unambiguously concluded that hydrogen bonds in the SPA are mainly formed by C=O and N-H bonds in pedants, as well as the hydroxyl groups.

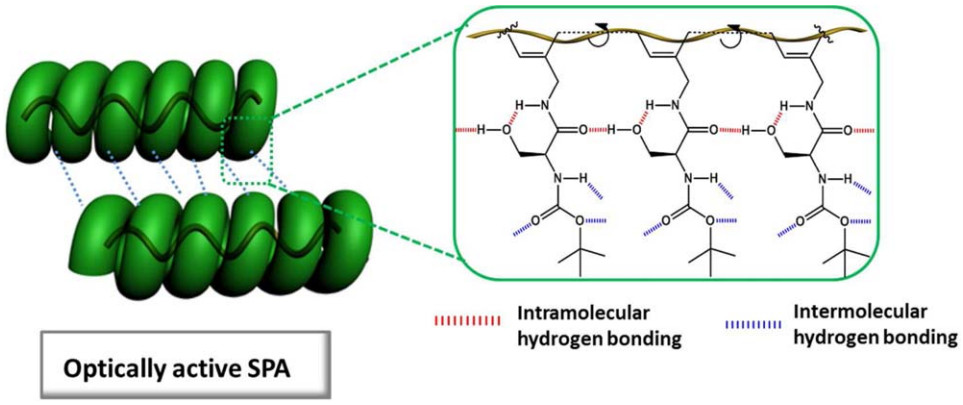

Figure 4. Hydrogen bonding and helical structure of the SPAs. [Color figure can be viewed in the online issue, which is available at wileyonlinelibrary.com.]

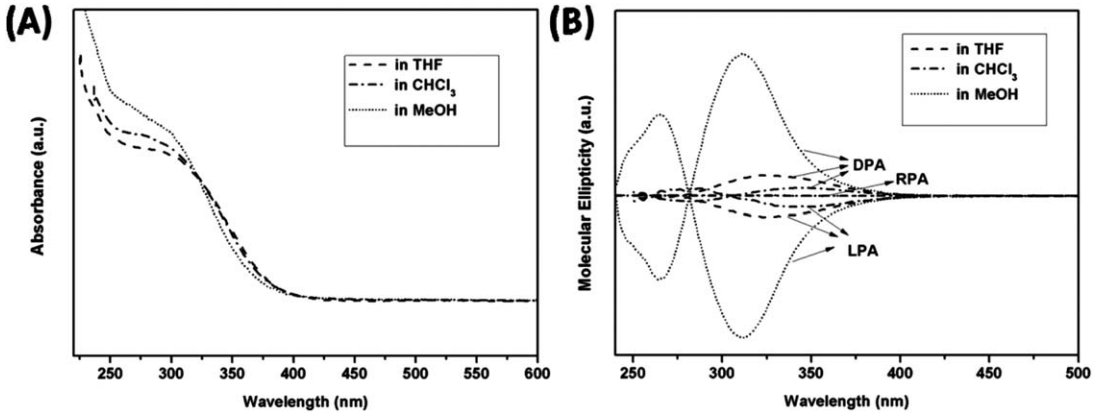

Figure 5. (A) UV-Vis spectra of LPA measured in different solvents; (B) CD spectra of LPA and DPA measured in different solvents. The concentration of measured sample is about 0.01 g dL^{-1}.

Optical Activity and Secondary Structure of SPAs

The conformation of SPA was examined by polarimetry along with UV-Vis and CD spectroscopic methods. LPA shows specific optical rotations of −152° (in $CHCl_3$, $c = 0.05$g dL^{-1}), −269° (in THF), and −456° (in MeOH), which largely depended on the solvents. The absolute values of $[\alpha]_D$ are about 25 to 76 times as large as that of monomer at the maximum, indicating the presence of chiral amplification in LPA. The large rotation values also demonstrate that the LPA macromolecule may take predominantly single-handed helical conformation in these three solvents. Similarly, DPA also shows large specific rotations in these solvents and the values of $[\alpha]_D$ are close to the opposite value of those of LPA. This suggests that DPA chain may also adopt a screw sense which is opposite to LPA. However, the RPA has no optical activity.

Figure 4 depicts the UV-Vis and CD spectra of LPA, DPA and RPA measured in different solvents at room temperature. As shown in Figure 4(A) and Supporting Information Figure S3, the three polymers almost have the same UV-Vis absorption. The broad absorption peak at ~320 nm corresponds to the transition of the π-conjunction in main chain of polyacetylene. In Figure 4(B), LPA exhibits negative intense CD signals at 347, 322, and 312 nm in chloroform, THF, and MeOH, respectively. The LPA and DPA exhibit similar strong Cotton effects with wonderful mirror image symmetry in same solvent. The results confirm that the SPAs based on L and D-serine are a couple of enantiomorphs which have the opposite single-handed helical conformation. On the contrary, RPA is CD inactive in any solvents which results from the random coiled polymer chain. Besides the obvious shift of CD peak positions, it can be also found that the CD intensity in $CHCl_3$ is relatively smaller than that in THF and MeOH, which agrees with the specific rotations. Since the helical conformation is likely to be stabilized by intramolecular hydrogen bonding along with steric repulsion, MeOH and THF as strong polar solvents can strongly influence asymmetric forces between substitutes and change the forming method of hydrogen bonds. In this case, MeOH may assist the LPA chain to take tighter and more stable helical conformation, because the hydroxyl groups in solvent can shield the inner amide groups by preventing them to form intramolecular hydrogen bonds with hydroxyl groups in pedants.[25] According to the difference in $[\alpha]_D$ values and CD spectra, it is not hard to assume that the hydroxyl groups in pedants participate in the formation of intramolecular hydrogen bonds and has significant effect in controlling and stabilizing the helix of optically active SPAs. Previous reports have pointed out that the amide-amide intramolecular hydrogen bonds significantly influence the formation of the secondary structure of SPAs carrying amino acid-based pedants.[28–30] The CD absorption at 390 to 400 nm of the previously reported poly(*N*-propargylamides) should be derived from their conjugated double bonds of the main chain. However, with regard to serine-derived SPAs, the CD absorption shifts to lower wavelength (<350 nm). Participation of hydroxyl group in the intramolecular amide-amide hydrogen bonding may be responsible for this phenomenon. Consequently, it is demonstrated that the dihedral angle at the single bond of the main chain of LPA and RPA is smaller, resulting in the decrease of conjugation length. The typical pitch in optically active SPA chain is schematically illustrated in Figure 5, although exact structure information is more complicated.

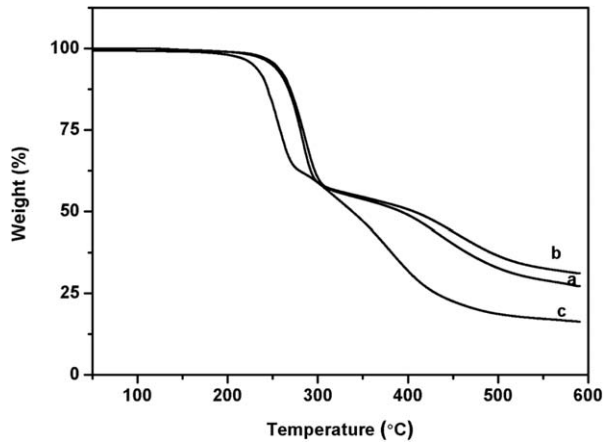

Figure 6. TGA curves of the samples: (A) LPA, (B) DPA, and (C) RPA.

Table III. Thermal Properties of SPAs in Nitrogen

Polymer	Decomposition temperature (°C) T_5	Decomposition temperature (°C) T_{10}
LPA	254	266
DPA	250	264
RPA	228	242

Thermal Properties

The thermal properties of SPAs were investigated by TGA techniques at a heating rate of 10°C min^{-1} under a nitrogen atmosphere. As can be seen in Figure 6, the TGA curve for each SPA product exhibit a smooth, stepwise manner, indicating a two-step thermal degradation. The thermogravimetric data of these SPAs are summarized in Table III. The onset temperatures of weight loss of the polymers were all above 200°C, indicating considerably high thermal stability of the SPAs. The temperature of 5% and 10% weight loss (T_5, T_{10}) of the SPAs have also been calculated by means of thermograms and used as criterion for evaluation of thermal stability of these SPAs (Table III). As we know, LPA, DPA, and RPA have the same chemical repeating units and approximate molecular weight, but their thermal stabilities are quite different. The T_5 value of RPA is around 228°C, whereas, LPA and DPA has a 5 wt % weight loss at the temperature of ~254°C. This indicates that optically active SPAs have higher thermal stability than the racemic polymer which may be due to more regulated secondary structures of LPA and

Table IV. Infrared Emissivity Values of SPAs Measured at Room Temperature

Polymer	Infrared emissivity (8–14 μm)
LPA	0.632
DPA	0.616
RPA	0.749

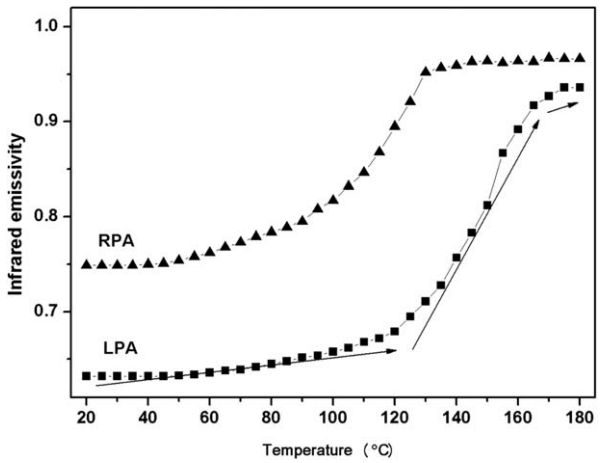

Figure 7. Infrared emissivity values of (A) LPA and (B) RPA at 20 to 180°C.

DPA. Moreover, the crystallinity of SPAs confirmed by the XRD is shown in Supporting Information Figure S4 and the polymers are amorphous.

Infrared Emissivity Study

The infrared emissivity values of the as-prepared SPAs at wavelength of 8 to 14 μm measured at room temperature are shown in Table IV. The infrared emissivity values of the PAs vary from 0.616 to 0.749. As mentioned above, the vibration of unsaturated groups in SPAs brings about high infrared emissivity values. Closely packed pitches in the polymers are favored over the decrease the index of hydrogen deficiency and the unsaturated degree, thus lowering the infrared emissivity. Empirical evidence has shown positive correlation between well-ordered and compact helical secondary structures and lower infrared emissivity values. LPA and DPA which adopt more orderly and compact helical conformation than RPA have proved to exhibit the lower infrared emissivity.

Furthermore, to further validate the effect of temperature on infrared emissivity properties, the infrared emissivity values of LPA and RPA measured from 20 to 180°C were tested and presented in Figure 7. From 20 to 120°C, the infrared emissivity value of LPA has increased slowly from 0.632 to 0.679; however, when the temperature is above 120°C, the value increases more rapidly to 0.693 at 160°C. These observations indicate that a large number of intramolecular hydrogen bonds have gradually disappeared above 120°C and the LPA chains are forced to adopt randomly coiled structures.[18,30] As the orderliness and helicity of LPA decrease rapidly, the infrared emissivity dramatically increases at a high speed. RPA also shows an increase of emissivity similar to LPA, but the inflectional point of temperature is not as obvious as LPA. This is because of the hydrogen bonds formed in RPA is less orderly and stable than optically active SPAs. These results also prove the importance of the hydrogen bonds in maintaining the secondary structure of the optically active SPAs.

CONCLUSIONS

In summary, we have designed and synthesized a series novel optically active SPAs derived from serine. The polymers carrying hydroxyl groups in the side chains have shown unique features in thermal properties and the optically active LPA and DPA are proved to adopt predominantly helical secondary structure. Systematic experimental investigations have been carried out to determine the roles of hydrogen bonding in stabilizing the helical structure of the SPAs. The infrared emissivity results show that the improvement of stablity and helicity of the helical structure in organic polymers significantly contributes to the decrease in infrared emissivity. Therefore, the incorporation of the chiral amino acid in as-prepared SPAs provides a great promise in the development of polymers with low infrared emissivity. Overall, the application of SPAs in reducing infrared emission in this paper is important not only because they exemplify extend application of helical polymers, but also because they provide a novel method to develop organic materials with low-emissivity.

ACKNOWLEDGMENTS

The authors are supported by National Nature Science Foundation of China (51077013), Fund Project for Transformation of Scientific and Technological Achievements of Jiangsu Province (No. BA2011086), the Fundamental Research Funds for the Central Universities and Innovation Research Foundation of College Graduate in Jiangsu Province (CXLX12-0107 and CXZZ13-0091), and the Scientific Research Foundation of Graduate School of Southeast University (YBJJ1417).

REFERENCES

1. Pan, C.; Zhang, J.; Yong, S. *Appl. Therm. Eng.* **2013**, *51*, 529.
2. Mahulikar, S. P.; Sonawane, H. R.; Rao, A. G. *Prog. Aerosp. Sci.* **2007**, *43*, 218.
3. Huang, Z.; Zhu, D.; Lou, F.; Zhou, W. *Appl. Surf. Sci.* **2008**, *255*, 2619.
4. Yan, X.; Xu, G. *J. Alloy Compd.* **2010**, *491*, 649.
5. Sun, K.; Zhou, W.; Tang, X.; Huang, Z.; Lou, F.; Zhu, D. *Appl. Surf. Sci.* **2011**, *257*, 9639.
6. Advincula, R. C. *J. Am. Chem. Soc.* **2011**, *133*, 5622.
7. Nakano, T.; Okamoto, Y. *Chem. Rev.* **2001**, *101*, 4013.
8. Masuda, T. *J. Polym. Sci. Part A: Polym. Chem.* **2007**, *45*, 165.
9. Furusho, Y.; Yashima, E. *Macromol. Rapid Commun.* **2011**, *32*, 136.
10. Wang, Z.; Zhou, Y.; Sun, Y.; Yao, Q. *Macromolecules* **2009**, *42*, 4972.
11. Yang, Y.; Zhou, Y.; Ge, J.; Yang, X. *React. Funct. Polym.* **2012**, *72*, 574.
12. Yang, Y.; Zhou, Y. M.; Ge, J. H.; Wang, Y. J.; Chen, X. L. *Polymer* **2011**, *52*, 3745.
13. Megens, R. P.; Roelfes, G. *Chem. Eur. J.* **2011**, *17*, 8514.
14. Lee, D.; Kim, H.; Suzuki, N.; Fujiki, M.; Lee, C. L.; Lee, W. E.; Kwak, G. *Chem. Commun.* **2012**, *48*, 9275.
15. Hu, Y.; Shiotsuki, M.; Sanda, F.; Masuda, T. *Chem. Commun.* **2007**, *0*, 4269.

16. Nomura, R.; Yamada, K.; Masuda, T. *Chem. Commun.* **2002**, *0*, 478.
17. Zhao, H.; Sanda, F.; Masuda, T. *Macromol. Chem. Phys.* **2006**, *207*, 1921
18. Zhao, H.; Sanda, F.; Masuda, T. *J. Macromol. Sci., Pure Appl. Chem.* **2007**, *44*, 389.
19. Cheuk, K. K. L.; Lam, J. W. Y.; Chen, J.; Lai, L. M.; Tang, B. Z. *Macromolecules* **2003**, *36*, 5947.
20. Li, B. S.; Lam, J. W. Y.; Yu, Z.-Q.; Tang, B. Z. *Langmuir* **2012**, *28*, 5770.
21. Zhao, H.; Sanda, F.; Masuda, T. *Macromolecules* **2004**, *37*, 8888.
22. Li, B. S.; Kang, S. Z.; Cheuk, K. K. L.; Wan, L.; Ling, L.; Bai, C.; Tang, B. Z. *Langmuir* **2004**, *20*, 7598.
23. Li, B. S.; Cheuk, K. K. L.; Salhi, F.; Lam, J. W. Y.; Cha, J. A. K.; Xiao, X.; Bai, C.; Tang, B. Z. *Nano Lett.* **2001**, *1*, 323.
24. Sanda, F.; Araki, H.; Masuda, T. *Macromolecules* **2004**, *37*, 8510.
25. Sanda, F.; Araki, H.; Masuda, T. *Macromolecules* **2005**, *38*, 10605.
26. Schrock, R. R.; Osborn, J. A. *Inorg. Chem.* **1970**, *9*, 2339.
27. Shiotsuki, M.; Sanda, F.; Masuda, T. *Polym. Chem.* **2011**, *2*, 1044.
28. Deng, J.; Tabei, J.; Shiotsuki, M.; Sanda, F.; Masuda, T. *Macromolecules* **2004**, *37*, 1891.
29. Sanda, F.; Gao, G.; Masuda, T. *Macromol. Biosci.* **2004**, *4*, 570.
30. Zhao, H.; Sanda, F.; Masuda, T. *Macromol. Chem. Phys.* **2005**, *206*, 1653.